

Syntheses, crystal structures and magnetic properties of one-, two- and three-dimensional 2,2'-bipyrimidine-containing copper(II) complexes

Giovanni De Munno,^{*a} Teresa Poerio,^a Miguel Julve,^{*†b} Francesc Lloret,^b Juan Faus^b and Andrea Caneschi^c

^a Dipartimento di Chimica, Università degli Studi della Calabria, 87030 Arcavacata di Rende, Cosenza, Italy

^b Departament de Química Inorgànica, Facultat de Química de la Universitat de València, Dr. Moliner 50, 46100 Burjassot (València), Spain

^c Dipartimento di Chimica, Università degli Studi di Firenze, Via Maragliano 77, 50144 Firenze, Italy

Three new copper(II) complexes of formula $[\text{Cu}(\text{bipym})(\text{H}_2\text{O})_2][\text{NO}_3]_2 \cdot \text{H}_2\text{O}$ **1**, $[\text{Cu}(\text{bipym})(\text{Cr}_2\text{O}_7)]$ **2** and $[\text{Cu}(\text{bipym})(\text{SO}_4)] \cdot \text{H}_2\text{O}$ **3** (bipym = 2,2'-bipyrimidine) have been synthesized and characterized by single-crystal X-ray diffraction. Compound **1** loses water very easily transforming into $[\text{Cu}(\text{bipym})][\text{NO}_3]_2$ **1'**. The structure of **1** consists of zigzag chains of bipym-bridged copper(II) ions with unco-ordinated nitrate anions and co-ordinated and crystallization water molecules, whereas the structures of **2** and **3** are made up of bipym-bridged copper(II) chains which are connected through bis(monodentate)-dichromate (**2**) and -sulfate (**3**) groups to yield sheet-like (**2**) and three-dimensional (**3**) polymers. The copper atom in compounds **1–3** exhibits a distorted elongated-octahedral co-ordination. In **1**, it is linked to two bis(chelating) bipym groups and two water molecules in *cis* positions. The equatorial positions of the octahedron are occupied by three bipym-nitrogen atoms and a water-oxygen, while the axial ones are filled by the remaining bipym-nitrogen and the second aqua ligand. The equatorial mean planes of two adjacent copper(II) ions within the chains are mutually perpendicular. In **2**, two different bis(chelating) bipym groups alternate regularly within the chain. The four nitrogen atoms of one of them build the equatorial positions of two neighbouring octahedra and the two remaining equatorial sites around each metal atom are filled by an oxygen atom of the dichromate group and a nitrogen atom of the second bipym. The two *trans* axial positions are occupied by another nitrogen atom of the second bipym and an oxygen atom of the dichromate anion. The two adjacent equatorial copper(II) mean planes through this second bridging bipym in **2** are mutually parallel. Two adjacent crystallographically independent metal atoms alternate regularly within the bipym-bridged copper(II) chain in **3**. Their equatorial plane is built by three nitrogen atoms from bipym and one oxygen atom from a sulfate anion, whereas the axial positions are filled by the remaining bipym nitrogen atom and an oxygen atom from another sulfate anion. The equatorial mean planes of adjacent copper(II) ions within the bipym-bridged chain of **3** are mutually perpendicular as in **1**. The metal–metal separations across bridging bipym are 5.646(1) Å in **1**, 5.486(2) and 5.765(2) Å in **2** and 5.648(1) and 5.715(1) Å in **3**, values which are close to that through bridging dichromate [5.774(1) Å in **2**] but shorter than those through bridging sulfate [6.464(2) and 6.417(2) Å in **3**]. Variable-temperature magnetic susceptibility measurements reveal that bridging bipym is able to mediate relatively strong (**1'** and **2**) and weak (**1** and **3**) antiferromagnetic couplings. The magnitude of the exchange coupling in this series is analyzed and discussed in the light of the complexes structural patterns.

The bis(chelating) co-ordination mode of 2,2'-bipyrimidine (bipym) allowed the preparation of a series of bipym-bridged dinuclear complexes of formula $[\text{M}_2(\text{bipym})]^{4+}$ where $\text{M} = \text{Zn}^{\text{II}}, \text{Cu}^{\text{II}}, \text{Ni}^{\text{II}}, \text{Co}^{\text{II}}, \text{Fe}^{\text{II}}$ or Mn^{II} .⁶ The intradimer magnetic coupling between the paramagnetic centers (the metal–metal separation across bipym being larger than 5.5 Å) along this series attains a maximum value of *ca.* -160 cm^{-1} in the copper(II) dimers and progressively decreases as the number of unpaired electrons on each metal site increases, being *ca.* -1 cm^{-1} in the manganese(II) compounds. In the light of these magneto-structural data, it is clear that bipym has a remarkable efficiency to transmit electronic effects at large distances when acting as a bridging ligand. Given that in this family of dimeric compounds water molecules complete the octahedral surrounding of the metal ions, systems with a greater nuclearity could be easily obtained by increasing the amount of bipym. Along this line, the zigzag chain compounds of formula $[\text{Cu}(\text{bipym})(\text{H}_2\text{O})_2][\text{ClO}_4]_2 \cdot \text{H}_2\text{O}$,⁷ $[\text{Co}(\text{bipym})(\text{H}_2\text{O})_2][\text{NO}_3]_2$,^{4c} $[\text{Fe}(\text{bipym})(\text{NCS})_2]$,⁸ $[\text{Mn}(\text{bipym})(\text{NO}_3)_2]$ ^{9,10} and $[\text{Mn}(\text{bipym})(\text{NCO})_2]$ ¹⁰ were obtained with a 1:1 metal to bipym molar ratio. Four

nitrogen atoms from two bipym ligands and two water molecules (Cu^{II} and Co^{II}), two thiocyanato-nitrogens (Fe^{II}) and either two cyanato-nitrogens or three nitrate-oxygens (Mn^{II}) in *cis* positions build a distorted octahedral environment [seven-co-ordination in the case of the manganese(II) nitrate chain].

In the framework of our current research of bipym-containing metal complexes, the influence of the nature of the counter ion on the polymerisation of the $[\text{Cu}(\text{bipym})]^{2+}$ unit in aqueous solution was investigated. This work allowed us to obtain one- (**1**), two- (**2**) and three-dimensional (**3**) bipym-containing copper(II) complexes of formula $[\text{Cu}(\text{bipym})(\text{H}_2\text{O})_2][\text{NO}_3]_2 \cdot \text{H}_2\text{O}$ **1**, $[\text{Cu}(\text{bipym})(\text{Cr}_2\text{O}_7)]$ **2** and $[\text{Cu}(\text{bipym})(\text{SO}_4)] \cdot \text{H}_2\text{O}$ **3**. The present contribution deals with their crystal structures as well as their magnetic properties as a function of temperature. The magnetic properties of the anhydrous phase of compound **1** $\{[\text{Cu}(\text{bipym})][\text{NO}_3]_2 \text{ 1'}\}$ are also reported.

Experimental

Materials

Copper(II) nitrate trihydrate, copper(II) sulfate pentahydrate, potassium chromate and 2,2'-bipyrimidine were obtained from

† E-Mail: miguel.julve@uv.es

commercial sources and used as received. Elemental analyses (C, H, N) were performed by the Microanalytical Service of the Università degli Studi della Calabria (Italy). Copper contents were determined by atomic absorption spectrometry.

Preparations

[Cu(bipym)(H₂O)₂][NO₃]₂·H₂O **1 and [Cu(bipym)][NO₃]₂ **1'**.** Parallelepiped blue-green crystals of **1** were obtained from aqueous solutions containing 1 mmol of Cu(NO₃)₂·3H₂O and 1 mmol of bipym by slow evaporation at room temperature. Owing to the great solubility of **1** in water, evaporation of the solvent nearly to dryness is required to obtain the product in a good yield (ca. 85%). The solid was filtered off and washed with a small amount of cold ethanol and diethyl ether (Found: C, 24.32; H, 2.98; Cu, 15.71; N, 20.93. Calc. for C₈H₁₂CuN₆O₉: C, 24.04; H, 3.03; Cu, 15.89; N, 21.02%). Complex **1** loses water (ca. 14% of weight, that is three water molecules per mol of copper) at room temperature under vacuum transforming into [Cu(bipym)][NO₃]₂ **1'**.

[Cu(bipym)(Cr₂O₇)] **2.** Prismatic brown single crystals of this compound were grown in aqueous solution by a slow-diffusion method using in an H-double-tube glass vessel. The starting solutions were aqueous solutions of [Cu(bipym)][NO₃]₂ (0.1 mmol) in one arm and K₂CrO₄ (0.2 mmol) in the other. On standing at room temperature, a few brown crystals of **1** appeared after 3 months mixed with a maroon powder. The crystals were picked and washed with some drops of cold water and dried on filter paper. The powder was filtered off, washed with water, ethanol and diethyl ether. Elemental analyses of this powder do not agree with the formula of **2** and it was discarded (Found: C, 21.82; H, 1.40; N, 12.75. Calc. for C₈H₆Cr₂CuN₄O₇: C, 21.95; H, 1.38; N, 12.80%). The occurrence of the equilibrium between dichromate and chromate in aqueous solutions of potassium chromate, the minority species being dichromate in neutral or basic medium, accounts for the formation of single crystals of **2**.

[Cu(bipym)(SO₄)₂·H₂O **3.** Prismatic green crystals of **3** were obtained from dilute aqueous solutions containing stoichiometric amounts of Cu(SO₄)₂·5H₂O and bipym by slow evaporation at room temperature. Complex **3** separates as a blue polycrystalline powder in quantitative yield by adding an ethanolic solution of bipym (1 mmol) to a concentrated aqueous solution of copper(II) sulfate (1 mmol) under stirring. The solid was filtered off and washed with a small amount of cold ethanol and diethyl ether (Found: C, 28.40; H, 2.45; Cu, 18.70; N, 16.63. Calc. for C₈H₈CuN₄O₅S: C, 28.62; H, 2.40; Cu, 18.93; N, 16.68%).

Physical techniques

The magnetic susceptibility measurements were carried out on polycrystalline samples of **1**, **1'**, **2** and **3** in the temperature range 2.0–300 K with Quantum Design (**1** and **1'**) and Metronique Ingenierie MS03 (**2** and **3**) SQUID magnetometers operating at 1 T. The polycrystalline sample of **1** was purged with helium during 15 min and quickly frozen to 2 K in order to avoid the loss of water. The heating mode was used in the magnetic study of this compound. The usual method (combination of helium purging and vacuum and the cooling mode) was used for the magnetic study of complexes **1'**, **2** and **3**; [NH₄]₂[Mn(SO₄)₂·6H₂O] was used as a calibrant. Diamagnetic corrections of the constituent atoms were estimated from Pascal's constants¹¹ and found to be -193×10^{-6} (**1**), -154×10^{-6} (**1'**), -171×10^{-6} (**2**) and -169×10^{-6} cm³ mol⁻¹ (**3**). Experimental susceptibilities were also corrected for the temperature-independent paramagnetism (-60×10^{-6} cm³ mol⁻¹ per Cu^{II}) and the magnetization of the sample holder.

Table 1 Summary of crystal data^a for [Cu(bipym)(H₂O)₂][NO₃]₂·H₂O **1**, [Cu(bipym)(Cr₂O₇)] **2** and [Cu(bipym)(SO₄)₂·H₂O **3**

Compound	1	2	3
Formula	C ₈ H ₁₂ CuN ₆ O ₉	C ₈ H ₆ Cr ₂ CuN ₄ O ₇	C ₈ H ₈ CuN ₄ O ₅ S
<i>M</i>	399.8	437.7	335.8
Crystal system	Monoclinic	Triclinic	Monoclinic
Space group	<i>Cc</i>	<i>P</i> $\bar{1}$	<i>Pn</i>
<i>a</i> /Å	10.073(2)	8.199(2)	8.868(2)
<i>b</i> /Å	16.372(3)	8.633(3)	13.752(3)
<i>c</i> /Å	9.746(2)	10.049(2)	9.848(2)
α /°		114.47(2)	
β /°	110.08(2)	92.67(2)	116.35(1)
γ /°		90.48(2)	
<i>U</i> /Å ³	1509.6(5)	646.4(3)	1076.2(4)
<i>Z</i>	4	2	8
<i>D</i> _c /g cm ⁻³	1.759	2.249	2.072
<i>F</i> (000)	812	430	676
μ (Mo-K α)/cm ⁻¹	15.1	33.2	22.5
<i>R</i> ^b	0.035	0.023	0.027
<i>R</i> ' ^c	0.038	0.029	0.029
<i>S</i> ^d	0.953	1.163	1.338

^a Details in common: *T* = 25 °C, *I* > 3 σ (*I*). ^b *R* = $\Sigma(|F_o| - |F_c|)/\Sigma|F_o|$. ^c *R*' = $[\Sigma w(|F_o| - |F_c|)^2/\Sigma w|F_o|^2]$. ^d Goodness of fit = $[\Sigma w(|F_o| - |F_c|)^2/(N_o - N_p)]^{1/2}$.

Crystallography

Crystals of dimensions 0.40 × 0.20 × 0.16 (**1**), 0.21 × 0.28 × 0.35 (**2**) and 0.42 × 0.28 × 0.23 mm (**3**) were mounted on a Siemens R3m/V automatic four-circle diffractometer and used for data collection. In order to avoid the loss of solvent from complex **1**, a single crystal was sealed in a Lindemann tube and then used for intensity data collection. Diffraction data were collected at room temperature using graphite-monochromated Mo-K α radiation ($\lambda = 0.71073$ Å) with the ω -2 θ scan method. The unit-cell parameters were determined from least-squares refinement of the setting angles of 25 reflections in the 2 θ range 15–30°. A summary of the crystallographic data and structure parameters for compounds **1–3** is given in Table 1. Examination of two standard reflections, monitored after every 148 reflections, showed no sign of crystal deterioration. Lorentz-polarization, extinction and absorption corrections¹² were applied to the intensity data. The maximum and minimum transmission factors were 0.681 and 0.620 for **1**, 0.491 and 0.455 for **2**, and 0.592 and 0.520 for **3**. Of the 1857 (**1**), 3271 (**2**) and 2694 (**3**) measured reflections in the 2 θ range 3–54° with index ranges $0 \leq h \leq 12$, $0 \leq k \leq 20$ and $-12 \leq l \leq 11$ (**1**), $0 \leq h \leq 10$, $-11 \leq k \leq 11$ and $-12 \leq l \leq 12$ (**2**) and $0 \leq h \leq 11$, $0 \leq k \leq 17$ and $-12 \leq l \leq 11$ (**3**), 1757 (**1**), 2842 (**2**) and 2530 (**3**) were unique. From these, 1340 (**1**), 2563 (**2**) and 2278 (**3**) were observed [*I* > 3 σ (*I*)] and used for the refinement of the structures.

The structures were solved by standard Patterson methods and subsequently completed by Fourier recycling. All non-hydrogen atoms, except the carbon-bipym atoms of complexes **1** and **3**, were refined anisotropically. The hydrogen atoms of the water molecules were located on a ΔF map and refined with constraints. The hydrogen atoms of bipym were set in calculated positions and refined as riding atoms with a common fixed isotropic thermal parameter. Full-matrix least-squares refinements were carried out by minimizing the function $\Sigma w(|F_o| - |F_c|)^2$ with $w = 1.000/[\sigma^2(F_o) + q(F_o)^2]$ where $q = 0.0012$ (**1**), 0.0010 (**2**) and 0.0004 (**3**). Models reached convergence with values of the *R* and *R*' indices listed in Table 1. All our attempts to refine the structures of complexes **1** and **3** in the corresponding centric space groups were unsuccessful due mainly to geometric molecular distortions. Criteria for satisfactory complete analysis were the ratios of the root mean square shift to standard deviation being less than 0.006 and no significant features in the final difference maps. The residual maxima

Table 2 Selected interatomic distances (Å) and angles (°) for compound **1** with estimated standard deviations (e.s.d.s) in parentheses^a

Cu(1)–O(1)	2.303(5)	Cu(1)–O(2)	1.969(5)
Cu(1)–N(1)	2.036(6)	Cu(1)–N(3)	2.024(9)
Cu(1)–N(2a)	2.049(8)	Cu(1)–N(4a)	2.397(6)
O(1)–Cu(1)–O(2)	88.1(2)	O(1)–Cu(1)–N(1)	87.2(2)
O(2)–Cu(1)–N(1)	171.0(2)	O(1)–Cu(1)–N(3)	98.6(2)
O(2)–Cu(1)–N(3)	92.0(2)	N(1)–Cu(1)–N(3)	81.2(3)
O(1)–Cu(1)–N(2a)	94.2(2)	O(2)–Cu(1)–N(2a)	93.0(3)
N(1)–Cu(1)–N(2a)	95.0(3)	N(3)–Cu(1)–N(2a)	166.4(2)
O(1)–Cu(1)–N(4a)	169.9(3)	O(2)–Cu(1)–N(4a)	92.1(2)
N(1)–Cu(1)–N(4a)	93.9(2)	N(3)–Cu(1)–N(4a)	91.5(3)
N(2a)–Cu(1)–N(4a)	75.7(3)		

Hydrogen bonds^b

A	D	H	A...D	A...H–D
O(3)	O(1)	H(2w)	2.79(1)	172(6)
O(8)	O(2)	H(3w)	2.78(1)	175(6)
O(9)	O(2)	H(4w)	2.61(1)	153(4)
O(6c)	O(1)	H(1w)	2.78(1)	159(6)
O(8d)	O(9)	H(6w)	2.88(1)	160(6)
O(5e)	O(9)	H(5w)	2.81(1)	160(6)

^a Symmetry code: a $x, -y, 0.5 + z$; c $-0.5 + x, 0.5 - y, -0.5 + z$; d $0.5 + x, 0.5 - y, 0.5 + z$; e $x, y, 1 + z$. ^b A = acceptor, D = donor.

Table 3 Selected interatomic distances (Å) and angles (°) for compound **2** with e.s.d.s in parentheses*

Cu(1)–N(1)	2.069(2)	Cu(1)–N(3)	2.014(2)
Cu(1)–O(6)	1.933(2)	Cu(1)–N(2b)	2.032(2)
Cu(1)–N(4a)	2.339(2)	Cu(1)–O(2c)	2.405(2)
N(1)–Cu(1)–N(3)	99.2(1)	N(1)–Cu(1)–O(6)	91.74(7)
N(3)–Cu(1)–O(6)	90.9(1)	N(1)–Cu(1)–N(2b)	81.1(1)
N(3)–Cu(1)–N(2b)	176.8(1)	O(6)–Cu(1)–N(2b)	88.7(1)
N(1)–Cu(1)–N(4a)	86.0(1)	N(3)–Cu(1)–N(4a)	76.6(1)
O(6)–Cu(1)–N(4a)	99.4(1)	N(2b)–Cu(1)–N(4a)	106.6(1)
N(1)–Cu(1)–O(2c)	84.1(1)	N(3)–Cu(1)–O(2c)	91.6(1)
O(6)–Cu(1)–O(2c)	92.6(1)	N(2b)–Cu(1)–O(2c)	85.3(1)
N(4a)–Cu(1)–O(2c)	163.2(1)		

* Symmetry code: a $-x, -y, 1 - z$; b $-x, 1 - y, 2 - z$; c $-x, 1 - y, 1 - z$.

and minima in the final Fourier-difference maps were 0.39 and -0.45 (**1**), 0.47 and -0.53 (**2**) and 0.39 and -0.49 e Å⁻³ (**3**). Solutions and refinements were performed with the SHELXTL PLUS system.¹³ The final geometrical calculations were carried out with the PARST program.¹⁴ Graphical manipulations were performed using the XP utility of the SHELXTL PLUS system. Main interatomic bond distances and angles are given in Tables 2 (**1**), 3 (**2**) and 4 (**3**).

CCDC reference number 186/941.

See <http://www.rsc.org/suppdata/dt/1998/1679/> for crystallographic files in .cif format.

Results and Discussion

Crystal structures

The structure of complex **1** consists of cationic chains of bipym-bridged copper(II) ions [Fig. 1(a)] of formula [Cu(bipym)(H₂O)₂]²⁺, unco-ordinated nitrate anions and lattice water molecules. The chains which are well separated from each other are linked through hydrogen bonds involving the nitrate counter ions and the co-ordinated and unco-ordinated water molecules [see Fig. 1(b) and end of Table 2]. The structures of complexes **2** and **3** are made up of similar bipym-bridged copper(II) chains [Figs. 2(a) and 3(a) for **2** and **3**, respectively] but without co-ordinated water molecules. These chains are joined by means of bis(monodentate)-dichromate (**2**) or -sulfate (**3**) groups to form two- [Fig. 2(b)] and three-dimensional [Fig.

Table 4 Selected interatomic distances (Å) and angles (°) for compound **3** with e.s.d.s in parentheses^a

Cu(1)–N(1)	1.971(7)	Cu(1)–N(3)	2.087(4)
Cu(1)–N(5)	2.073(7)	Cu(1)–N(7)	2.442(5)
Cu(1)–O(1)	1.952(4)	Cu(1)–O(2c)	2.266(4)
Cu(2)–N(2)	2.383(4)	Cu(2)–N(4)	2.068(6)
Cu(2)–O(5)	1.940(4)	Cu(2)–N(6a)	2.093(4)
Cu(2)–N(8a)	2.003(7)	Cu(2)–O(6d)	2.298(4)
N(1)–Cu(1)–N(3)	80.1(2)	N(1)–Cu(1)–N(5)	172.0(2)
N(3)–Cu(1)–N(5)	94.0(2)	N(1)–Cu(1)–N(7)	99.3(2)
N(3)–Cu(1)–N(7)	86.3(2)	N(5)–Cu(1)–N(7)	74.7(2)
N(1)–Cu(1)–O(1)	93.9(2)	N(3)–Cu(1)–O(1)	168.8(2)
N(5)–Cu(1)–O(1)	91.0(2)	N(7)–Cu(1)–O(1)	85.3(1)
N(1)–Cu(1)–O(2c)	93.5(2)	N(3)–Cu(1)–O(2c)	88.1(1)
N(5)–Cu(1)–O(2c)	91.8(2)	N(7)–Cu(1)–O(2c)	164.9(2)
O(1)–Cu(1)–O(2c)	101.8(1)	N(2)–Cu(2)–N(4)	75.8(2)
N(2)–Cu(2)–O(5)	79.1(1)	N(3)–Cu(2)–O(5)	90.3(2)
N(2)–Cu(2)–N(6)	85.0(1)	N(4)–Cu(2)–N(6a)	96.0(2)
O(5)–Cu(2)–N(6a)	173.5(2)	N(2)–Cu(2)–N(8a)	95.6(2)
N(4)–Cu(2)–N(8a)	170.9(2)	O(5)–Cu(2)–N(8a)	93.7(2)
N(6a)–Cu(2)–N(8a)	80.2(2)	N(2)–Cu(2)–O(6d)	160.6(2)
N(4)–Cu(2)–O(6d)	91.6(2)	O(5)–Cu(2)–O(6d)	96.6(1)
N(6)–Cu(2)–O(6d)	81.8(2)	N(8a)–Cu(2)–O(6d)	96.0(2)

Hydrogen bonds^b

A	D	H	A...D	A...H–D
O(6)	O(9)	H(2w)	2.85(1)	159(4)
O(4)	O(10)	H(4w)	2.82(1)	168(6)
O(1c)	O(10)	H(3w)	2.85(1)	153(5)
O(8d)	O(9)	H(1w)	2.89(1)	135(4)

^a Symmetry code: a $x, y, 1 + z$; c $0.5 + x, -y, 0.5 + z$; d $0.5 + x, 1 - y, 0.5 + z$. ^b A = Acceptor, D = donor.

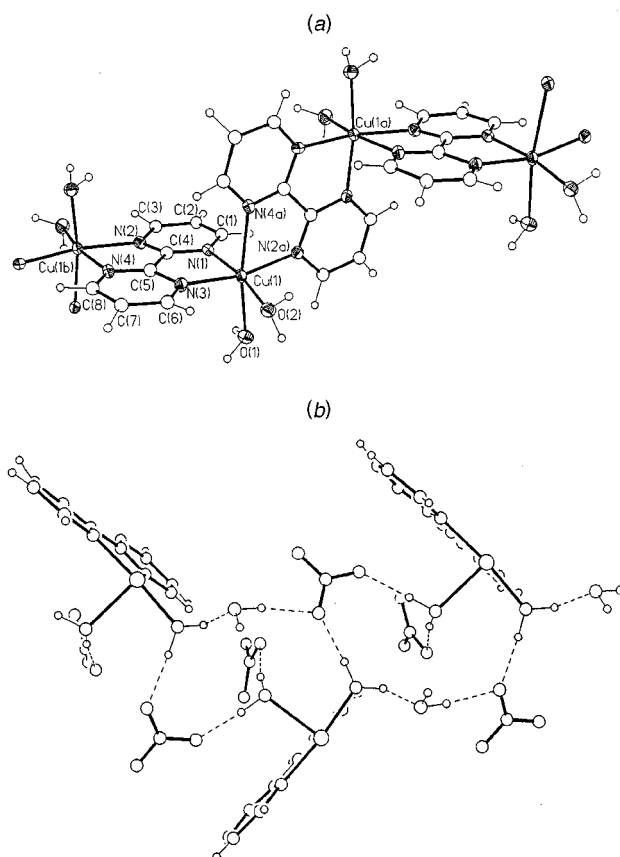


Fig. 1 (a) A perspective view of the cationic chain [Cu(bipym)(H₂O)₂]²⁺ of complex **1** along the z axis, showing the atom numbering scheme. All carbon atoms are drawn with uniform arbitrarily sized circles. Thermal ellipsoids of the remaining atoms are drawn at the 30% probability level. (b) A view of the xy plane of complex **1** that illustrates the hydrogen-bonding interactions (broken lines) linking unco-ordinated nitrate and co-ordinated and crystallization water molecules

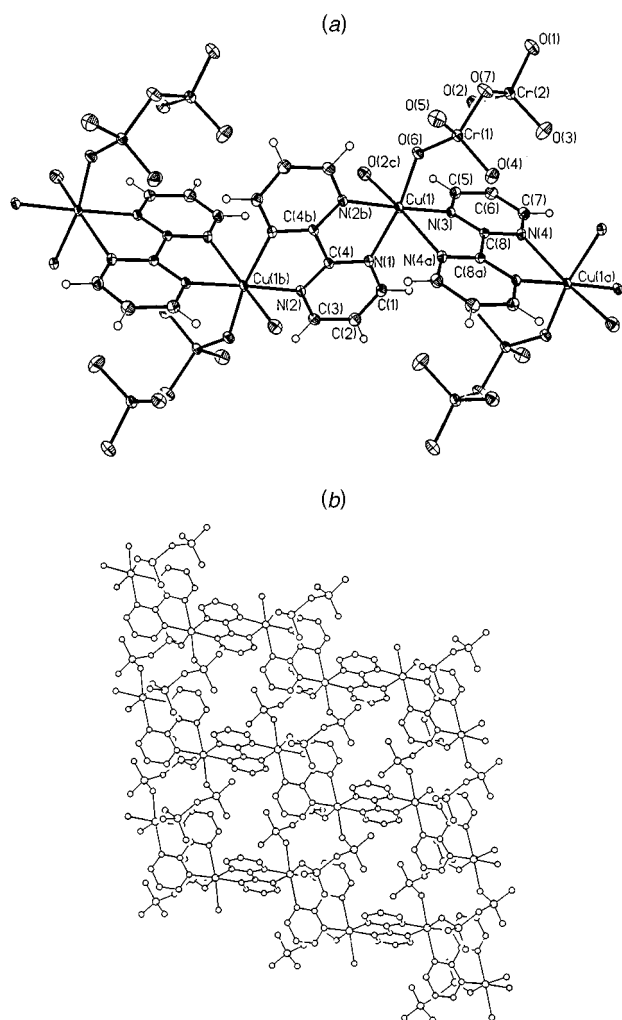


Fig. 2 (a) A perspective view of the asymmetric unit and one symmetry-related unit of complex **2** with the atom numbering. Thermal ellipsoids are drawn at the 30% probability level. (b) A view of the *xz* plane of the structure of complex **2** showing its two-dimensional nature

3(b)] polymers. Crystallization water molecules contribute to the packing forming hydrogen bonds in complex **3** (see end of Table 4).

Each metal atom in complex **1** is in a distorted octahedral environment being linked to two bipym ligands and two water molecules in *cis* positions. The equatorial positions of the octahedron are occupied by three bipym-nitrogen [N(1), N(2a) and N(3)] and one water-oxygen [O(2)] atoms, whereas the axial ones are filled by the remaining bipym-nitrogen [N(4a)] and the second water-oxygen [O(1)] atoms. The largest deviation from the mean equatorial plane is 0.047(7) Å for N(4a) and the copper atom is 0.041(1) Å out of this plane. The adjacent equatorial mean planes within the chain are mutually perpendicular. This structure is similar to that reported for the compound of formula [Cu(bipym)(H₂O)₂][ClO₄]₂·H₂O **4**⁷ where the nitrate has been replaced by perchlorate. The average equatorial Cu–N bond distance in **1** is 2.036(8) Å, a value somewhat longer than the Cu(1)–O(2) bond length, 1.969(5) Å. These values compare well with those reported for **4** [2.04(1) and 2.001(9) Å for Cu–N and Cu–O bonds, respectively]. As far as the axial bonds are concerned, the differences are more significant: the Cu–N bond length is longer in **1** [2.397(6) Å] than in **4** [2.330(10) Å], while the opposite trend is exhibited by the Cu–O bonds [2.303(5) (1) and 2.325(11) Å (4)].

All copper atoms in complex **2** are equivalent and exhibit an elongated octahedral geometry. Two different bis(chelating) bipym groups alternate regularly within the bipym-bridged copper(II) chain in contrast to what occurs in **1** where all bipym

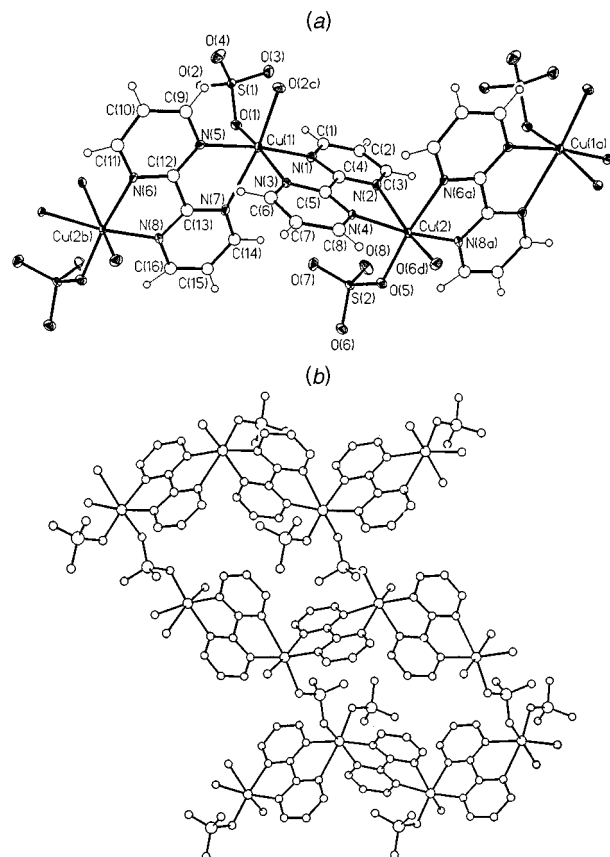


Fig. 3 (a) A perspective view of the asymmetric unit and one symmetry-related unit of complex **3** with the atom numbering. All carbon atoms are drawn with uniform arbitrarily sized circles. Thermal ellipsoids are plotted at the 30% probability level. (b) A view of the three-dimensional arrangement in complex **3** through bridging bipym and sulfate groups

ligands are equivalent. The bipym ligand containing the N(1), N(2), N(1b) and N(2b) set of atoms is bound to the copper atoms [Cu(1) and Cu(1b)] through four short bonds, whereas the other one with N(3), N(4), N(3a) and N(4a) forms two short [Cu(1)–N(3) and Cu(1a)–N(3a)] and two long [Cu(1)–N(4a) and Cu(1a)–N(4)] bonds. The four nitrogen atoms of the first bipym group occupy the equatorial positions of two neighbouring octahedra, an inversion centre being located at the middle of the C(4)–C(4b) bond. The two remaining equatorial sites are filled by an oxygen atom of the dichromate group [O(6)] and one nitrogen atom [N(3)] of the second bipym ligand. Also an inversion centre stands at the middle of the C(8)–C(8a) bond of this second bipym ensuring two short and two long metal-to-bipym bonds mutually *trans*. Six co-ordination is achieved by means of the remaining nitrogen atom [N(4a)] of this second bipym molecule and another oxygen atom [O(2c)] of the dichromate group. The three equatorial Cu–N (bipym) bond lengths average 2.038(2) Å, a value which is somewhat longer than the equatorial Cu–O bond [1.933(2) Å for Cu(1)–O(6)]. Both values are significantly shorter than the axial Cu–N [2.339(2) Å] and Cu–O [2.405(2) Å] bond lengths. The best equatorial plane around Cu(1) is built by the N(1), N(2b), N(3) and O(6) atoms, the largest deviation from this mean plane being 0.003(2) Å for N(2b). The copper atom is displaced by 0.052(1) Å from this plane towards N(4a). The equatorial planes around Cu(1) and Cu(1a) are parallel whereas those around Cu(1) and Cu(1b) are coplanar.

Two crystallographically independent copper atoms [Cu(1) and Cu(2)] are present in the structure of compound **3** in contrast to what is observed in the structures of the complexes **1** and **2**. They are both octahedrally distorted: two different bis(chelating) bipym molecules and two oxygen atoms from two

sulfate groups in *cis* positions build the co-ordination polyhedron around the copper atom. The best equatorial planes around Cu(1) and Cu(2) which are defined by the N(1), N(3), N(5) and O(1) [Cu(1)] and N(4), N(6a), N(8a) and O(5) [Cu(2)] set of atoms, are mutually perpendicular as in compound **1**. The N(7) and O(2c) [Cu(1)] and N(2) and O(6d) [Cu(2)] atoms occupy the axial positions. The Cu–O equatorial distances [1.952(4) and 1.940(4) Å for Cu(1)–O(1) and Cu(2)–O(5), respectively] are somewhat shorter than the remaining Cu–N equatorial bonds {average values 2.044(6) [Cu(1)] and 2.055(6) Å [Cu(2)]}. They are significantly shorter than the axial ones [2.442(5) and 2.266(4) Å for Cu(1)–N(7) and Cu(1)–O(2c) and 2.383(4) and 2.298(4) Å for Cu(2)–N(2) and Cu(2)–O(6d)]. The largest deviations from the mean equatorial planes around the copper atoms are 0.042(5) Å at N(1) [Cu(1)] and 0.120(5) Å at N(8a) [Cu(2)]. The copper atoms are displaced from these mean planes by 0.142(1) [Cu(1)] and 0.042(1) Å [Cu(2)].

The pyrimidyl rings of the bipym molecules in **1–3** are planar as expected, the largest deviations from the mean planes being not greater than 0.013(7) (**1**), 0.015(3) (**2**) and 0.017(6) Å (**3**). The bipym ligands as a whole are almost planar [the dihedral angles between the pyrimidine rings are 5.1(2)° (**1**), 0° (**2**), and 0.5(1)° and 2.2(2)° (**2**)]. The Cu(1) and Cu(1b) atoms in **1** and Cu(1) in **2** are 0.082(1) and 0.101(1) Å (**1**) and 0.173(1) Å (**2**) out of the mean bipym planes. In compound **3**, Cu(1) and Cu(2) are 0.103(1) and 0.324(1) Å out of the N(1)⋯N(2) bipym plane, whereas Cu(1) and Cu(2b) are only 0.072(1) and 0.037(1) Å out of the N(5)⋯N(6) bipym plane. The angles subtended at the metal atom by the bipym ligand vary in two different ranges, 74.7(2)–76.6(1)° and 80.1(2)–81.2(3)° depending on whether bipym is bound to copper through a short and a long or two short bonds, respectively. The dihedral angles between the mean adjacent bipym planes are 93.2(1)° (**1**), 89.4(1)° (**2**) and 90.0(1)° (**3**).

The unco-ordinated nitrate in complex **1** has its expected trigonal geometry. The nitrogen–oxygen bond lengths and the intra-anion bond angles average 1.23(1) Å and 120.0(7)°, respectively. The co-ordinated sulfate anions in compound **3** are tetrahedral, as expected with sulfur–oxygen bond lengths and intra-anion bond angles averaging 1.472(5) Å and 109.4(3)°. The significant lengthening of the S(1)–O(1) [1.507(4) Å] and S(2)–O(5) [1.519(4) Å] bonds is due to their co-ordination to copper through short equatorial bonds *via* O(1) and O(5) atoms {the remaining S–O bond lengths vary in the ranges 1.450(6)–1.461(7)° [S(1)] and 1.449(6)–1.478(4)° [S(2)]}. Each chromium atom in compound **2** exhibits a slightly distorted tetrahedral geometry. The two tetrahedral CrO₄ groups are joined by a shared O(7) oxygen atom forming a dichromate anion in an almost eclipsed conformation. The Cr(1)–O(7)–Cr(2) bridging angle is 125.1(1)°, a value which is in the range of previously reported dichromate-containing compounds.^{15,16} The bridging Cr–O bonds are 1.759(2) and 1.803(2) Å for Cr(1)–O(7) and Cr(2)–O(7), respectively. They are longer than the terminal Cr–O ones, where the maximum and minimum bond lengths are 1.675(2) [Cr(1)–O(6)] and 1.596(2) Å [Cr(1)–O(5)] and 1.623(2) [Cr(2)–O(2)] and 1.603(2) Å [Cr(2)–O(3)]. Within the terminal Cr–O bonds, a significant lengthening is observed for the values of the Cr(1)–O(6) and Cr(2)–O(2) bonds because of the co-ordination of dichromate to copper(II) through the O(6) (equatorial position) and O(2) (axial position) oxygen atoms.

The metal–metal separation across bridging bipym in **1** is 5.646(1) Å, to be compared with 5.597(3) Å in compound **4**. The shortest interchain metal–metal distance in **1** is much longer [7.792(1) Å for Cu(1)⋯Cu(1c) and Cu(1)⋯Cu(1d)] than the intrachain one in **1**. There are two different metal–metal separations across the bridging bipym in complex **2**, 5.486(2) and 5.765(2) Å for Cu(1)⋯Cu(1b) and Cu(1)⋯Cu(1a), respectively. The fact that one bipym is bound to two copper atoms [Cu(1) and Cu(1b)] through four short bonds whereas the other one forms one short and one long

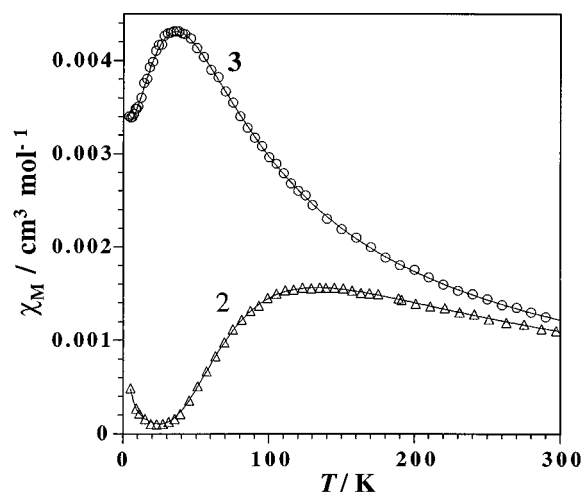


Fig. 4 Temperature dependence of the molar magnetic susceptibility for compounds **2** (Δ) and **3** (\circ); the continuous lines are the best fits (see text)

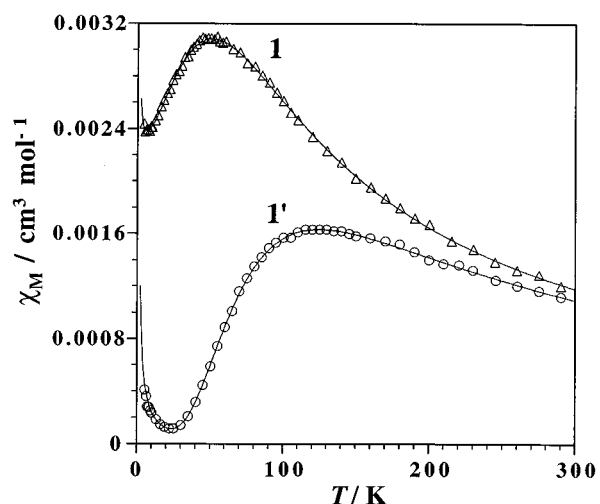
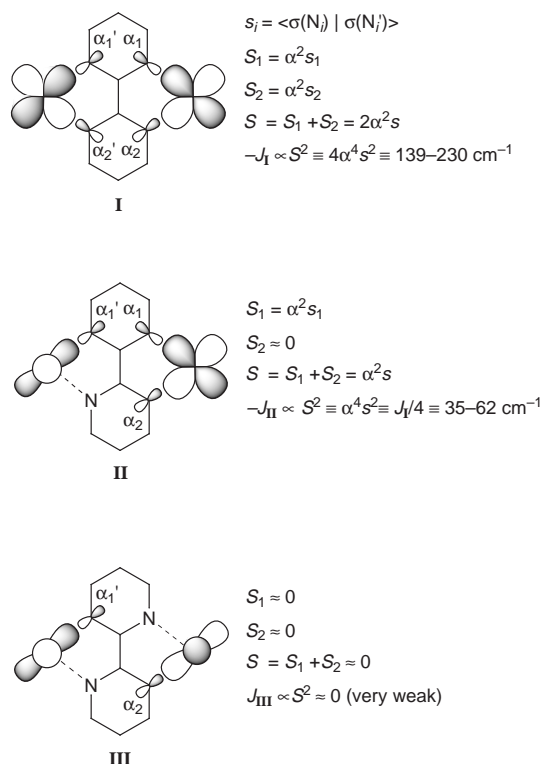


Fig. 5 Temperature dependence of the molar magnetic susceptibility for compounds **1** (Δ) and **1'** (\circ); the continuous lines are the best fits (see text)

bond on each side [Cu(1) and Cu(1a)], accounts for these structural features. The metal–metal separation through bridging dichromate is 5.774(1) Å [Cu(1)⋯Cu(1c)] whereas the shortest intersheet metal–metal distance is 8.199(2) Å [Cu(1)⋯Cu(1d)]. In compound **3**, two nearly equal metal–metal separations across bridging bipym occur: 5.648(1) and 5.715(19) Å for Cu(1)⋯Cu(2) and Cu(2)⋯Cu(1a), respectively. The copper–copper separations through bridging sulfate are somewhat longer, 6.417(2) [Cu(2)⋯Cu(2d) and Cu(2)⋯Cu(2f)]; (f) = $x - 0.5, 1 - y, z - 0.5$] and 6.464(2) Å [Cu(1)⋯Cu(1c) and Cu(1)⋯Cu(e)]; (e) = $x - 0.5, -y, z - 0.5$].

Magnetic properties

The plots of the magnetic susceptibility per mol of copper(II) (χ_M) versus T for complexes **1–3** exhibit susceptibility maxima at 50 (**1**), 120 (**1'**), 135 (**2**) and 35 K (**3**) and they are characteristic of an antiferromagnetic interaction between local doublets. The magnetic susceptibility curves for complexes **2** and **3** are depicted in Fig. 4 whereas that for complexes **1** and **1'** are shown in Fig. 5. Small amounts of monomeric impurities account for the increase of χ_M in the low temperature region. It should be noted that the susceptibility curves for complexes **1** and **1'** are very close to those of compounds **2** and **3**, respectively. The values of $\chi_M T$ at room temperature are 0.36 (**1**), 0.34 (**1'**), 0.33 (**2**) and 0.38 cm³ mol⁻¹ K (**3**). These values decrease when cooling and vanish at $T = 0$ K.



Scheme 1 Magnetic coupling schemes in complexes **1–3**; s_i is the overlap integral between $\sigma(N_i)$ and $\sigma(N_i')$ orbitals

The analysis of the magnetic properties of this family of complexes requires a detailed inspection of their structures in order to choose the most appropriate model. Compounds **1–3** have in common the occurrence of bipym-bridged copper(II) chains. In the case of complexes **2** and **3**, these chains are linked through bis(monodentate)-dichromate (**2**) and -sulfate (**3**) to yield two- (**2**) and three-dimensional (**3**) copper(II) networks. Focusing on the structures of **2** and **3**, one can see that both dichromate and sulfate adopt an asymmetrical bis(monodentate) co-ordination mode occupying one equatorial position around the metal atom [O(6) in **2** and O(1) and O(5) in **3**] and an axial one on the symmetry related metal center [O(2c) in **2** and O(2c) and O(6d) in **3**]. Keeping in mind such structural features, a significant spin density of copper(II) will be delocalized on the equatorial oxygen atom of dichromate [O(6)] or sulfate [O(1) and O(5)] but practically no spin density will be present on the symmetry-related dichromate [O(2c)] or sulfate [O(2c) and O(6d)] axial oxygen atoms. The lack of significant spin overlapping through bridging dichromate or sulfate with these structural patterns would lead to a very weak magnetic coupling between the copper(II) ions involved. Consequently, in spite of their two (**2**) and three-dimensional (**3**) structures, the magnetic coupling observed in these two complexes should be mainly mediated by bridging bipym.

We have proceeded to interpret the coupling through the bipym bridge by using the model of interaction of localized nonorthogonal magnetic orbitals by Kahn and Briat.¹⁷ We recall that in the context of this model, the value of the exchange coupling J for a dinuclear bipym-bridged copper(II) unit is proportional to the square of the overlapping integral (S) between the two mainly copper centred magnetic orbitals.^{7b,18} An inspection of the bipym-bridged copper(II) chain in **2** and **3** reveals significant differences. Two different centrosymmetric bis(chelating) bipym alternate regularly within the chain in complex **2**, one forming two short Cu–N bonds on each side (**I**, α is the mixing coefficient of the bipym-nitrogen in the magnetic orbital), whereas the other forms one short and one long bond on each side (**III**). In the light of the previous magneto-structural data concerning bipym-bridged copper(II)

compounds,^{7b,19} the magnetic behaviour of complex **2** should correspond to an alternating chain with alternating strong (**I**) and weak (**III**) antiferromagnetic couplings. In the case of complex **3**, each bipym form two short bonds with one copper atom on one side and one short and one long with the other copper atom on the other side in such a way that the overlapping between the copper(II) centred magnetic orbitals is only important on one side of the bridge, as illustrated by **II**. Given that two slightly structural different bridging bipym alternate within the bipym–copper(II) chain in **3**, the magnetic behaviour of **3** should be described also through an alternating chain model but the value of the alternating parameter (α) should be very close to one. Consequently, the magnetic data of complexes **2** and **3** were fitted to an antiferromagnetic Heisenberg $S = \frac{1}{2}$ alternating chain model²⁰ through the Hamiltonian $\hat{H} = -J \sum (\hat{S}_{2i} \cdot \hat{S}_{2i-1} + \alpha \hat{S}_{2i} \cdot \hat{S}_{2i+1})$. The values of J , α , g , ρ and R are -147 cm^{-1} , 0.03, 2.1, 0.45 and 4×10^{-5} for **2** whereas they are -38 cm^{-1} , 0.95, 2.09, 0.30 and 7×10^{-5} for **3**. The percentage of monomeric impurities per mol of copper atom (assuming that the molecular weight of the impurity is the same as that of the investigated compound) is given by ρ and R is the agreement factor defined as $R = \sum_i [(\chi_M)_{\text{obs}}(i) - (\chi_M)_{\text{cal}}(i)]^2 / \sum_i [(\chi_M)_{\text{obs}}(i)]^2$. Given that the alternating parameter for complex **2** is very small in agreement with the information summarized in **I** and **III**, we have also analyzed its magnetic behaviour through a simple Bleaney–Bowers expression for a dinuclear copper(II) complex and the results of the fit are -149 cm^{-1} , 2.1, 0.45 and 5×10^{-5} for J , g , ρ and R , respectively. The value of the antiferromagnetic coupling through the σ in-plane pathway (**I**) is practically identical in both approaches and the quality of the fit does not allow us to distinguish between them. The fact that for complex **3** the value of α is very close to unity, caused us to analyze its magnetic behaviour through the empirical expression of the magnetic susceptibility proposed by Estes *et al.*²¹ to fit antiferromagnetic Heisenberg copper(II) uniform chains ($\hat{H} = -J \sum \hat{S}_i \cdot \hat{S}_{i+1}$). The results of the fit are $J = -39 \text{ cm}^{-1}$, $g = 2.09$, $\rho = 0.30$ and $R = 8 \times 10^{-5}$. In the light of this result the uniform chain model for **3** seems as appropriate as that of the alternating chain. It is quite satisfying to note that the relatively strong antiferromagnetic coupling through bridging bipym from **I** (compound **2**) is roughly four times that observed through bridging bipym from **II** (compound **3**), as predicted by simple symmetry considerations, and that both values agree with that previously reported for related compounds.

In the case of complex **1**, we are dealing with a uniform copper(II) chain where the bis(chelating) bipym exhibits the same co-ordination mode as that observed in the structure of **3** (**III**). A similar magnetic coupling is thus expected in agreement with the similarity between their magnetic susceptibility curves. The analysis of its magnetic behaviour through the empirical expression to fit antiferromagnetic Heisenberg copper(II) uniform chains leads to values of -55 cm^{-1} , 2.1, 0.25 and 7.2×10^{-5} for J , g , ρ and R , respectively. This J value is somewhat greater than that of complex **3** (-39 cm^{-1}) and close to that of **4** (-62 cm^{-1}). The shortening of the Cu–N (bipym) bonds within the Cu–N–C–N–Cu exchange pathway [average Cu–N bond distance of 2.08 (**3**) and 2.04 Å (**1**, **4**)] accounts for the slightly stronger antiferromagnetic coupling in **1** and **4**. The magnetic curve of complex **1'** (Fig. 5), that is the anhydrous phase of complex **1**, is very close to that of complex **2**. This feature strongly suggests the formation of the pair in **1'** through a nitrate-assisted loss of water, the overall structure of **1'** being probably similar to that of complex **2**. In this respect, it deserves to be noted that carboxylate-assisted loss of water molecules in terephthalate-bridged metal complexes with the subsequent formation of carboxylate-bridged pairs accounted for the enhancement of the antiferromagnetic coupling observed for this family of compounds after dehydration.²² The magnetic data of **1'** fit well the simple Bleaney–Bowers expression for a dinuclear copper(II) complex with J , g , ρ and R values of -140

cm⁻¹, 2.08, 0.60 and 8.1×10^{-5} , respectively. The lack of structural data for this compound does not allow us to go further in our discussion.

We would like to finish the present contribution with some comments about the great variety of the structural possibilities issued from the bipym-containing copper(II) complexes by using the copper-to-bipym molar ratio and the nature of the counter ion (or coligand) as variables. The lowest copper-to-bipym molar ratio represented by the [Cu₂(bipym)]⁴⁺ unit has been isolated as a dimer by using negatively charged species which can act as counter ions (sulfate)^{2c} or end-cap ligands (croconate or squarate).^{2a,b} This dinuclear species has been used also as a suitable building block in designing chains with alternating ferro- (through double-hydroxo bridges) and antiferromagnetic (through bridging bipym) interactions,^{23,24} alternating magnetic planes^{19,25-27} and three-dimensional networks.^{19b} The species with 1:1 copper-to-bipym molar ratio, that is [Cu(bipym)]²⁺, also offers diverse synthetic possibilities depending on the chelating or bis(chelating) co-ordination mode that bipym can adopt for this stoichiometry. When it acts as a chelating group, the mononuclear [Cu(bipym)][ox]·7H₂O²⁵ (ox = oxalate dianion) or dinuclear [Cu₂(bipym)₂(OH)₂]X₂·6H₂O (X = ClO₄⁻ or NO₃⁻)^{24,28} complexes are isolated, whereas if it exhibits the bis(chelating) co-ordination mode, the present work shows that the dimensionality can be increased from one to three (complexes 1-3). Finally, the 2:3 Cu^{II}-to-bipym molar ratio leads to dinuclear species containing both chelating and bis(chelating) bipym groups^{7b} and higher molar ratios yield only mononuclear compounds.^{7b,29,30}

Acknowledgements

Financial support from the Dirección General de Investigación Científica y Técnica (DGICYT) (Spain) through Project PB94-1002 and the Italian Ministero dell'Università e della Ricerca Scientifica e Tecnologica is gratefully acknowledged.

References

- 1 G. De Munno and M. Julve, *Acta Crystallogr., Sect. C*, 1994, **50**, 1034.
- 2 (a) I. Castro, J. Sletten, L. K. Glærum, F. Lloret, J. Faus and M. Julve, *J. Chem. Soc., Dalton Trans.*, 1994, 2777; (b) I. Castro, J. Sletten, L. K. Glærum, J. Cano, F. Lloret, J. Faus and M. Julve, *J. Chem. Soc., Dalton Trans.*, 1995, 3207; (c) G. De Munno, M. Julve, F. Lloret, J. Cano and A. Caneschi, *Inorg. Chem.*, 1995, **34**, 2048.
- 3 G. De Munno, M. Julve, F. Lloret and A. Derory, *J. Chem. Soc., Dalton Trans.*, 1993, 1179.
- 4 (a) G. Brewer and E. Sinn, *Inorg. Chem.*, 1985, **24**, 4580; (b) G. De Munno, M. Julve, F. Lloret, J. Faus and A. Caneschi, *J. Chem. Soc., Dalton Trans.*, 1994, 1175; (c) G. De Munno, M. Julve, F. Lloret, T. Poerio and G. Viau, *New J. Chem.*, in the press.
- 5 J. A. Real, J. Zarembowitch, O. Kahn and X. Solans, *Inorg. Chem.*, 1987, **26**, 2939; E. Andrés, G. De Munno, M. Julve, J. A. Real and F. Lloret, *J. Chem. Soc., Dalton Trans.*, 1993, 2169; J. Sletten, H. Daraghme, F. Lloret and M. Julve, *Inorg. Chim. Acta*, in the press.
- 6 G. De Munno, R. Ruiz, F. Lloret, J. Faus, R. Sessoli and M. Julve, *Inorg. Chem.*, 1995, **34**, 408; D. M. Hong, Y. Y. Chu and H. H. Wei, *Polyhedron*, 1996, **15**, 447.
- 7 (a) L. W. Morgan, K. V. Goodwin, W. T. Pennington and J. D. Petersen, *Inorg. Chem.*, 1992, **31**, 1103; (b) G. De Munno, M. Julve, M. Verdagner and G. Bruno, *Inorg. Chem.*, 1993, **32**, 2215.
- 8 G. De Munno, M. Julve, J. A. Real, F. Lloret and R. Scopelliti, *Inorg. Chim. Acta*, 1996, **250**, 81.
- 9 D. M. Hong, H. H. Wei, L. L. Gan, G. H. Lee and Y. Wang, *Polyhedron*, **15**, 2335.
- 10 G. De Munno, T. Poerio, M. Julve, F. Lloret, G. Viau and A. Caneschi, *J. Chem. Soc., Dalton Trans.*, 1997, 601.
- 11 A. Earnshaw, *Introduction to Magnetochemistry*, Academic Press, London, New York, 1968.
- 12 N. Walker and D. D. Stuart, *Acta Crystallogr., Sect. A*, 1983, **39**, 158.
- 13 SHELXTL PLUS, Version 4.21/V, Siemens Analytical X-Ray Instruments Inc., Madison, WI, 1990.
- 14 M. Nardelli, *Comput. Chem.*, 1983, **7**, 95.
- 15 P. Martín-Zarza, P. Gili, F. V. Rodríguez-Romero and C. Ruiz-Pérez, *Polyhedron*, 1995, **14**, 2907 and refs. therein.
- 16 J. Mestres, M. Durán, P. Martín-Zarza, E. Medina de la Rosa and P. Gili, *Inorg. Chem.*, 1993, **32**, 4708 and refs. therein.
- 17 O. Kahn and B. Briat, *J. Chem. Soc., Faraday Trans. 2*, 1976, **72**, 268.
- 18 J. J. Girerd, M. F. Charlot and O. Kahn, *Mol. Phys.*, 1977, **34**, 1063; O. Kahn and M. F. Charlot, *Nouv. J. Chim.*, 1980, **4**, 567.
- 19 (a) M. Julve, G. De Munno, G. Bruno and M. Verdagner, *Inorg. Chem.*, 1988, **27**, 3160; (b) M. Julve, M. Verdagner, G. De Munno, J. A. Real and G. Bruno, *Inorg. Chem.*, 1993, **32**, 795.
- 20 O. Kahn, *Molecular Magnetism*, VCH, New York, 1993, p. 263.
- 21 W. E. Estes, D. P. Gavel, W. E. Hatfield and D. J. Hodgson, *Inorg. Chem.*, 1978, **17**, 1415.
- 22 J. Cano, G. De Munno, J. L. Sanz, R. Ruiz, J. Faus, F. Lloret, M. Julve and A. Caneschi, *J. Chem. Soc., Dalton Trans.*, 1997, 1915.
- 23 M. L. Kirk, W. E. Hatfield, M. S. Lah, D. Kessissoglou, V. L. Pecoraro, L. W. Morgan and J. D. Petersen, *J. Appl. Phys.*, 1991, **69**, 6013.
- 24 G. De Munno, M. Julve, F. Lloret, J. Faus, M. Verdagner and A. Caneschi, *Angew. Chem., Int. Ed. Engl.*, 1993, **32**, 1046; *Inorg. Chem.*, 1995, **34**, 157.
- 25 G. De Munno, M. Julve, F. Nicoló, F. Lloret, J. Faus, R. Ruiz and E. Sinn, *Angew. Chem., Int. Ed. Engl.*, 1993, **32**, 613.
- 26 G. De Munno, J. A. Real, M. Julve, M. C. Muñoz, *Inorg. Chim. Acta*, 1993, **211**, 227.
- 27 S. Decurtins, H. W. Schmalle, P. Schneuwly, L. M. Zheng, J. Ensling and A. Hauser, *Inorg. Chem.*, **34**, 5501.
- 28 I. Castro, M. Julve, G. De Munno, G. Bruno, J. A. Real, F. Lloret and J. Faus, *J. Chem. Soc., Dalton Trans.*, 1992, 1739.
- 29 G. De Munno, G. Bruno, M. Julve and M. Romeo, *Acta Crystallogr., Sect. C*, 1990, **46**, 1828.
- 30 R. R. Ruminiski, *Inorg. Chim. Acta*, 1985, **103**, 159.

Received 24th November 1997; Paper 7/08477C